



Spectroscopic Characterization of Nickel Based Foils

Zeynep AYGUN^{1,*}

¹ Vocational School of Technical Sciences, Bitlis Eren University, Bitlis, 13000, Turkey, **ORCID:** 0000-0002-2979-0283

Article Info

Research paper

Received : January 21, 2019

Accepted : April 30, 2019

Keywords

Foil Alloy
Nickel-based
Spectroscopic Analysis
Structural Study

Abstract

In this research, we carried out some structural and magnetic analyses of foil alloys in the form of Ni_xCr_{1-x} ($x=0.8$); $Ni_xCu_yFe_z$ ($x=0.65$, $y=0.33$, $z=0.02$); $Ni_xFe_yCu_zMo_t$ ($x=0.77$, $y=0.14$, $z=0.05$, $t=0.04$); $Ni_xCr_yCo_z(MoTiAlFe)_t$ ($x=0.58$, $y=0.19$, $z=0.14$, $t=0.09$) and $Ni_xCo_yCr_zFe_w(NMoMn)_w$ ($x=0.13$, $y=0.425$, $z=0.20$, $t=0.20$, $w=0.045$). In order to have knowledge about the magnetic properties, we use electron paramagnetic resonance spectroscopy which is effective to see the paramagnetism in the structure. For structural analyses, several techniques were studied. Fourier transform infrared spectrophotometer was performed to understand the functional groups in the structures. Raman experiment was applied for determination of molecular contents and mineralogy of the samples. Energy dispersive spectroscopy was used to learn the elemental compositions of the foils. The surface morphologies were seen by scanning electron microscopy. The obtained magnetic, structural and elemental results of the nickel based foil alloys are discussed in detail.

1. Introduction

Alloy is a material obtained by using two or more metals in various proportions with different preparation procedures. In this way, alloys can be used to reduce cost of material by preserving or changing some important properties, which is the reason why they have been used in a wide variety of applications [1]. Therefore, in many studies, alloys with different contents and preparation methods have taken part in previous studies [1-4]. A magnetic alloy is an integration of various metals that contains at least one of the three main magnetic elements: iron (Fe), nickel (Ni), or cobalt (Co). Alloys which are based on nickel, consist of at least 50% content of nickel, are of interest due to the uses in different areas such as aerospace engines, marine equipment, nuclear reactors, and petrochemical industries. The nickel-based alloys containing about 79% Ni have high initial and maximum permeabilities and very low hysteresis losses. Additions of 4-5% Mo, copper or chromium to 79% Ni-Fe alloy, have made the alloy interesting and the magnetic characteristics of the structures important [2].

In this work, our aim is to study the nickel-based foil alloys, which have diverse considerable features and various applications. For this purpose, we used spectroscopic techniques to characterize the alloys and to give enlightening information. Electron Paramagnetic Resonance (EPR) Spectroscopy that is an effective tool for detecting paramagnetic species in the structures with the presence of external magnetic field is used for magnetic investigation. A point, line and area scan, qualitative and quantitative analyzes in these areas can be determined by Energy Dispersive Spectroscopy (EDS) method. Fourier Transform Infrared Spectrophotometer (FTIR) is applied for learning functional groups. Raman Spectroscopy (RS) is used to get molecular contents, and Scanning Electron Microscopy (SEM) is preferred for surface morphology. To the best of our knowledge, no paper in the literature addresses this kind of topic, therefore, reporting the EPR, FTIR, Raman, EDS, and SEM analyses of the Ni-based foils will be useful.

2. Materials and Methods

In the present study, we provided our alloys commercially in foil form from Goodfellow Corporation.

* Corresponding Author: zeynepyarbasi@hotmail.com



EPR spectra of foil samples were recorded by X-band EPR spectrometer (≈ 9.25 GHz) with 100 kHz modulation field at room temperature. The scanning electron microscope images of alloys were recorded by Zeiss Sigma 300 SEM Spectrometer. Bruker VERTEX 70v was used to get FTIR results. WITech alpha 300R was operated for Raman analysis.

3. Results and Discussion

In the research, we investigated 5 different nickel based alloys in the foil form to learn the magnetic behaviors in an external magnetic field and structural features by several spectroscopic techniques.

Electron paramagnetic resonance is an operative technique commonly used to determine the local chemical environment of nuclei which is magnetically active ($I \neq 0$), paramagnetic species or radicals that have one or more unpaired electrons in the forms of biological or chemical structures. Various locations of ions assembled within the glassy matrix or within crystalline phases (oxides, silicates, titanates, etc.), which can not be determined with elementary analysis, can be examined by EPR. The EPR signals identified by g-values are calculated from the equation $h\nu = g\beta H$ with H the magnetic field, ν the microwave frequency, h the Planck constant and β the electron Bohr magneton. Room temperature EPR experiment is carried out for Ni based foil alloys and obtained spectra are given in Figure 1.

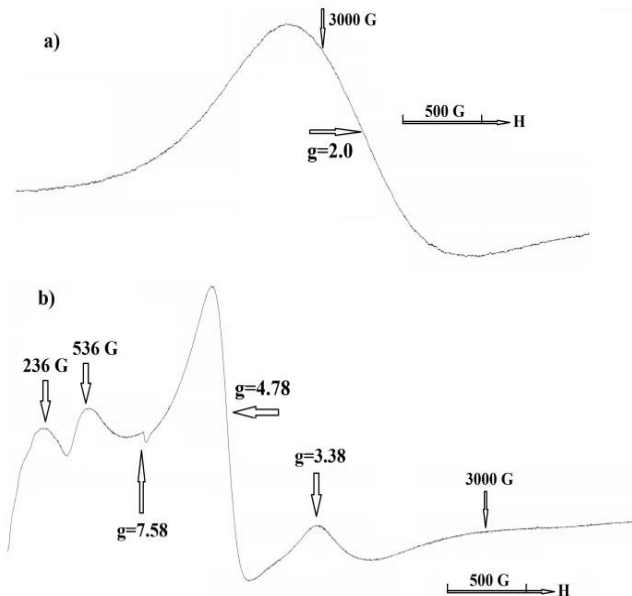


Figure 1. EPR spectra of a) $\text{Ni}_{0.65}\text{Cu}_{0.33}\text{Fe}_{0.02}$ b) $\text{Ni}_{0.77}\text{Fe}_{0.14}\text{Cu}_{0.05}\text{Mo}_{0.04}$ alloys recorded at room temperature.

We can conclude from the spectra that only $\text{Ni}_x\text{Cu}_y\text{Fe}_z$ and $\text{Ni}_x\text{Fe}_y\text{Cu}_z\text{Mo}_t$ samples are EPR active. Any EPR signal are not obtained for other three foil alloys. In the EPR spectrum of $\text{Ni}_x\text{Cu}_y\text{Fe}_z$ (Figure 1a), we saw a signal with a g-value of ≈ 2.0 which can be attributed to Fe^{+3} ions form clusters of several units in the structure or associated with a low ferric spin state [5]. Reddy et al. [6] also reported that the resonance signal at $g \approx 2.049$ is a characteristic of Cu^{2+} ion. As given in Fig. 1b, $\text{Ni}_x\text{Fe}_y\text{Cu}_z\text{Mo}_t$ alloy has more than one EPR signal with g-values of 3.38; 4.78; 7.58 and >9 . According to the previous studies, the lines with g values of ≈ 4.78 and ≈ 7.58 can be labeled as the lines of Fe^{+3} ions (Fe_2O_3) [7,8]. The $g > 9$ value was related to Fe(II) center by Delineau et al. [9]. Magnetite (Fe_3O_4) is a ferrimagnetic compound and seen as a broad EPR signal at low magnetic field less than 1000 G [10]. The broadening of EPR signals can be arisen from the dipole-dipole and exchange interaction between the interacting spins. An EPR line at $g \approx 3.7$ was reported as a FeMo protein signal before [11].

Raman spectroscopy studies are widely carried out for material identification and substances analysis. Generally, Raman and FTIR techniques are performed together to make investigation easily. Raman spectra obtained for five samples are given in Figure 2.

As reported by Kumar et al., Fe_3O_4 and $\alpha\text{-Fe}_2\text{O}_3$ show similar crystal structure and can not be distinguished by some techniques [12]. Raman spectroscopy is used for detailed analysis of iron oxide. Bands located at 656 and 303 cm^{-1} were assigned to magnetite (Fe_3O_4) [13]. Bands around 220, 250 and 500 cm^{-1} can be attributed to hematite (Fe_2O_3) centers [14]. Peaks at about 221, 287, 401, 493, and 601 cm^{-1} (200–800 cm^{-1}) defined the peaks for $\alpha\text{-Fe}_2\text{O}_3$ and we observe these peaks for the samples [15]. Wang et al. reported that peak at 660 cm^{-1} can be the representation of the existence of Fe_3O_4 [15]. This peak at around 660 cm^{-1} is seen for our $\text{Ni}_x\text{Cr}_{1-x}$; $\text{Ni}_x\text{Fe}_y\text{Cu}_z\text{Mo}_t$; $\text{Ni}_x\text{Cr}_y\text{Co}_z(\text{MoTiAlFe})_t$ and $\text{Ni}_x\text{Co}_y\text{Cr}_z\text{Fe}_t(\text{NMoMn})_w$ samples. Neale et al. mentioned a weak band at 537 cm^{-1} which can be ascribed with the Ni-O stretching mode [16]. This peak is also identical signal for the NiO_x layer on Ni metal surfaces. We observe this peak at around 530 cm^{-1} for the samples. The resonant peak at 1550 cm^{-1} is assigned to Co which was also observed by Yoon et al. for cobalt metal [17]. For samples containing Co, we are able to see this peak. In general, the obtained peaks for Raman spectra are compatible with other experimental results. The line intensities can be changeable related with the concentrations of the elements and the ingredients of the samples.

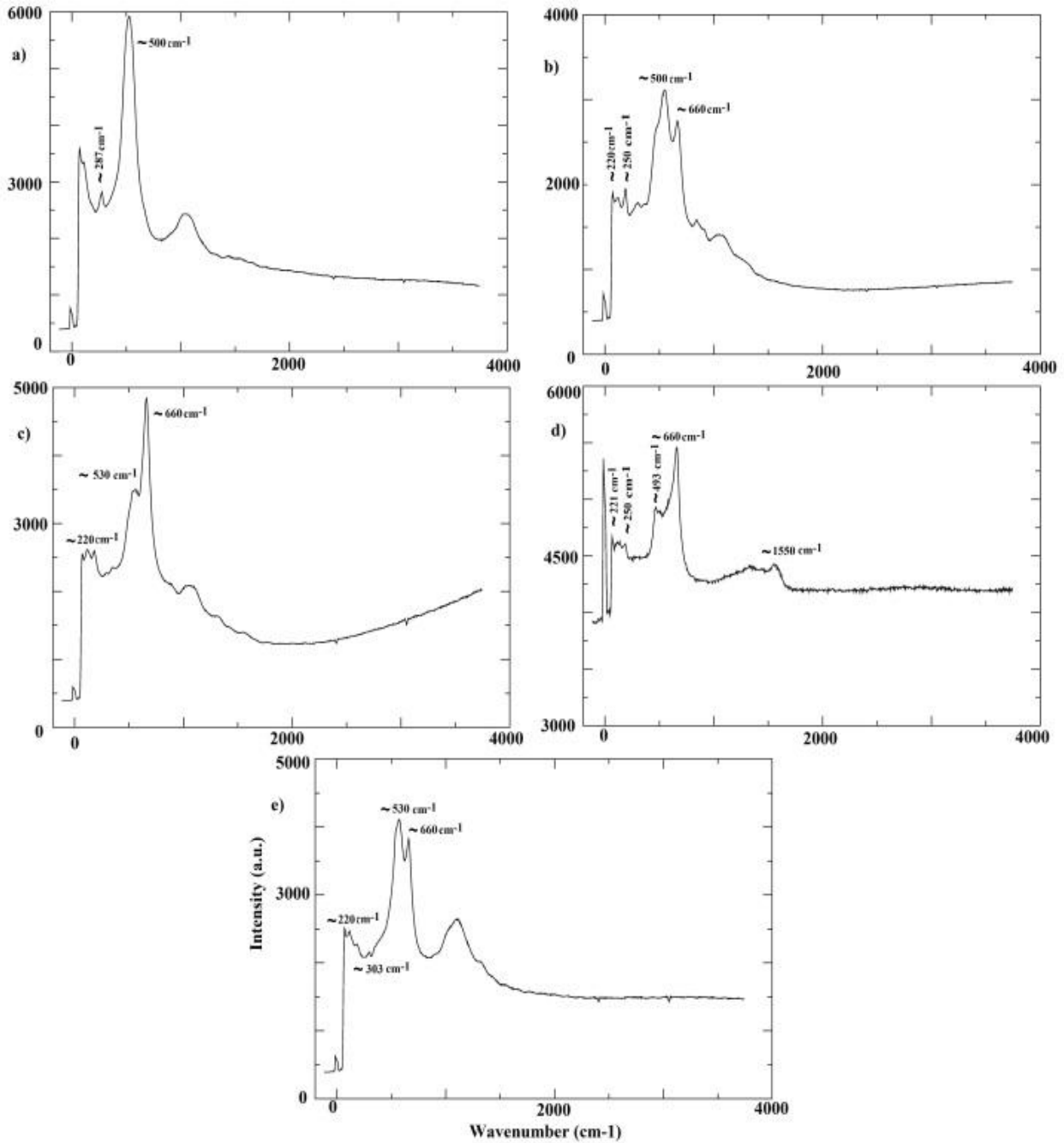


Figure 2. Raman spectra of a) $\text{Ni}_{0.65}\text{Cu}_{0.33}\text{Fe}_{0.02}$ b) $\text{Ni}_{0.77}\text{Fe}_{0.14}\text{Cu}_{0.05}\text{Mo}_{0.04}$ c) $\text{Ni}_{0.58}\text{Cr}_{0.19}\text{Co}_{0.14}(\text{MoTiAlFe})_{0.09}$ d) $\text{Ni}_{0.13}\text{Co}_{0.425}\text{Cr}_{0.20}\text{Fe}_{0.20}(\text{NMnMn})_{0.045}$ e) $\text{Ni}_{0.80}\text{Cr}_{0.20}$ alloys recorded at room temperature.

In Figure 3, FTIR spectra obtained at room temperature of five nickel-based alloys are shown. For all samples, we are able to see same bands around 600 cm^{-1} ascribed with large crystals of hematite (Fe_2O_3) which can be seen in different forms in the structures [18]. Peaks can be also seen around 170 and 250 cm^{-1} that were assigned to

magnetite (Fe_3O_4) centers [18]. Generally, the peaks of the structures are similar due to the similar ingredients (with some differences). The intensities of the peaks differ because of the amounts of the elements. We can observe some overlaps due to the presence of other components.

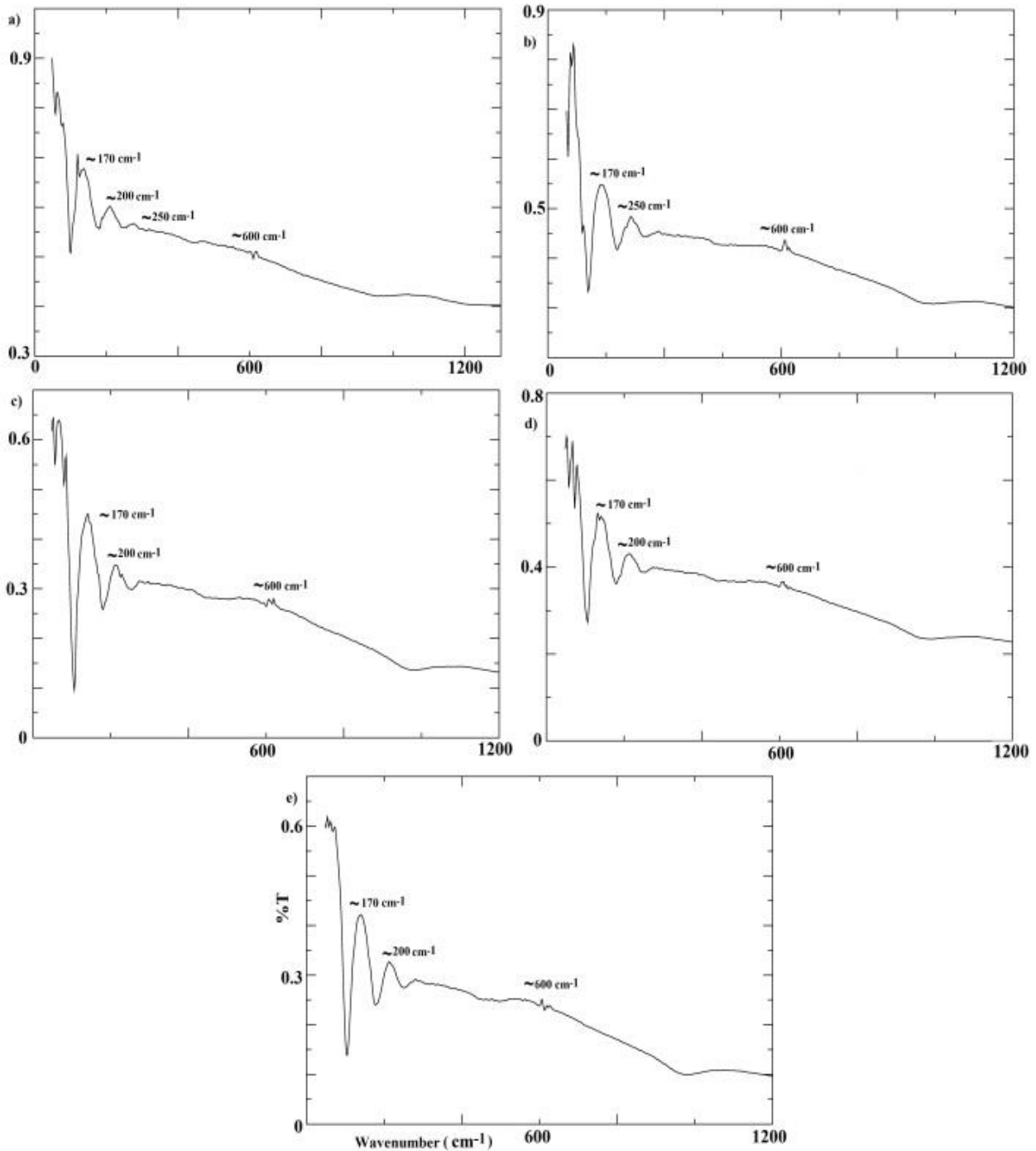


Figure 3. FTIR spectra of a) $\text{Ni}_{0.65}\text{Cu}_{0.33}\text{Fe}_{0.02}$ b) $\text{Ni}_{0.77}\text{Fe}_{0.14}\text{Cu}_{0.05}\text{Mo}_{0.04}$ c) $\text{Ni}_{0.58}\text{Cr}_{0.19}\text{Co}_{0.14}(\text{MoTiAlFe})_{0.09}$ d) $\text{Ni}_{0.13}\text{Co}_{0.425}\text{Cr}_{0.20}\text{Fe}_{0.20}(\text{NMoMn})_{0.045}$ e) $\text{Ni}_{0.80}\text{Cr}_{0.20}$ alloys recorded at room temperature.

SEM photographs of foil alloys recorded at room temperature to see the surface morphology are shown in Figure 4.

As shown in the images, all samples give

homogenous, smooth surfaces with parallel grooves. Some micro crystallites are seen on the surfaces. Elemental compositions of the five samples are investigated by EDS at room temperature and obtained values are given in Table 1.

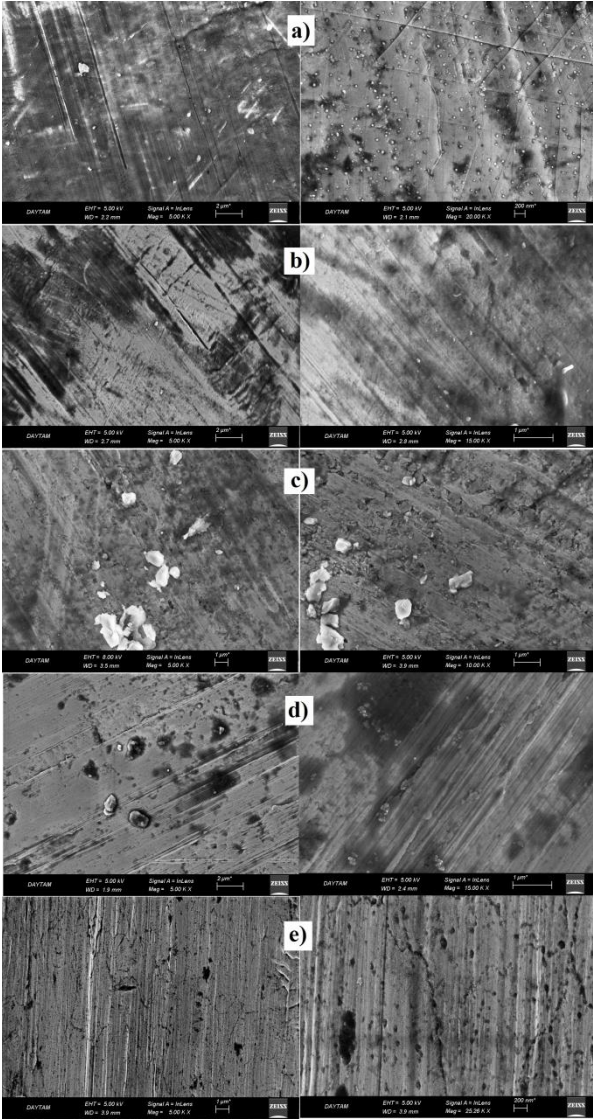


Figure 4. SEM images of a) $Ni_{0.65}Cu_{0.33}Fe_{0.02}$
 b) $Ni_{0.77}Fe_{0.14}Cu_{0.05}Mo_{0.04}$
 c) $Ni_{0.58}Cr_{0.19}Co_{0.14}(MoTiAlFe)_{0.09}$
 d) $Ni_{0.13}Co_{0.425}Cr_{0.20}Fe_{0.20}(NMoMn)_{0.045}$
 e) $Ni_{0.80}Cr_{0.20}$ alloys recorded at room temperature.

Table 1. EDS results obtained for a) $Ni_{0.65}Cu_{0.33}Fe_{0.02}$
 b) $Ni_{0.77}Fe_{0.14}Cu_{0.05}Mo_{0.04}$
 c) $Ni_{0.58}Cr_{0.19}Co_{0.14}(MoTiAlFe)_{0.09}$
 d) $Ni_{0.13}Co_{0.425}Cr_{0.20}Fe_{0.20}(NMoMn)_{0.045}$
 e) $Ni_{0.80}Cr_{0.20}$ alloys at room temperature.

	a)	b)	c)	d)	e)
	%Wt				
Fe	1.79	12.36	1.37	19.88	-
Ni	64.09	80.36	67.55	14.93	83.98
Cu	34.13	6.18	-	-	-
Mo	-	1.11	1.13	0.76	-
Co	-	-	13.06	45.62	-
Cr	-	-	14.77	17.21	16.02
Al	-	-	0.24	-	-
Ti	-	-	1.88	-	-
Mn	-	-	-	1.60	-

4. Conclusions

In the present study, we investigated five foil alloys based on nickel by using several spectroscopic techniques. By room temperature EPR experiment, we did not obtain any paramagnetic result for Ni_xCr_{1-x} ; $Ni_xCr_yCo_z(MoTiAlFe)_t$ and $Ni_xCo_yCr_zFe_t(NMoMn)_w$. So, these alloys are EPR inactive. For $Ni_xCu_yFe_z$ and $Ni_xFe_yCu_zMo_t$ samples, we were able to see EPR lines attributed to ferric centers. Raman investigations of the alloys showed the molecular contents, and supported the EPR results by giving some ferric peaks with different intensities due to the different amounts of elements. From FTIR results, we were able to see the functional groups. The peaks obtained by FTIR had different intensities, too. SEM images gave the surface morphologies and elemental compositions were presented by EDS technique.

Acknowledgements

SEM, EDS, Raman and FTIR results were obtained from the center of East Anatolia High Technology Application and Research Center (DAYTAM). EPR results were obtained from Advanced Technology Research & Application Center (ILTEK).

References

- [1] Aygun Z., Aygun M., Han I., 2018. Magnetic and Structural Analysis of Cu_xNi_{1-2x} and $Cu_yNi_zMn_{1-2y-2z}$ Alloys Using EPR, XRD and SEM Methods. Iranian Journal of Science and Technology Transaction Science, **42**, 951–957.
- [2] Aygun Z., 2018. Application of Spectroscopic Methods for Analysis of Ni-Based Alloys (Ni% ≥ 70). Cumhuriyet Science Journal, **39**, 144-151.
- [3] Alim B., Ugurlu M., Han İ., Demir L., 2018. Investigation of Alloying Effects on XRF Parameters of 3D Transition Metals in Permendur49, Kovar and Ti50Co50 Alloys. Journal of Radiation Research and Applied Sciences, **11**, 144-149.
- [4] Han I., Demir L., 2009. Valence-electron Configuration of Fe, Cr, and Ni in Binary and Ternary Alloys from K-to-K X-ray Intensity Ratios. Physical Review A, **80**, 1-6.
- [5] Symmons M. C. R., Peterson R. L., 1978. Electron Capture by Oxyhemoglobin: An ESR Study. Proceedings of the Royal Society B, **201**, 285-300.
- [6] Reddy A. J., Kokila M. K., Nagabhushana H., Chakradhar R. P. S., Shivakumara C., Rao J. L., Nagabhushana B. M., 2011. Structural, Optical and

- EPR Studies on ZnO:Cu Nanopowders Prepared via Low Temperature Solution Combustion Synthesis. *Journal of Alloys and Compounds*, **509**, 5349–5355.
- [7] Prakash C., Husain S., Singh R. J., Mollah S., 2001. Electron Paramagnetic Resonance of Fe Ions in BiO–PbO–Fe₂O₃ glasses. *Journal of Alloys and Compounds*, **326**, 47–49.
- [8] Ikeya M., 1993. *New Applications of ESR Dating Dosimetry Microscopy*; eds: Zimmerman M. R., Whitehead N., Singapore.
- [9] Delineau T., Allard T., Muller J. P., Barges D., Yvon J., Cases J. M., 1994. FTIR Reflectance vs. EPR Studies of Structural Iron in Kaolinites. *Clays and Clay Mineralogy*, **3**, 308-320.
- [10] Ledoux F., Zhilinskaya E. A., Courcot D., Aboukais A., Puskaric E., 2004. EPR Investigation of Iron in Size Segregated Atmospheric Aerosols Collected at Dunkerque, Northern France. *Atmospheric Environment*, **38**, 1201–1210.
- [11] Davis L. C., Henzl M. T., Burris R. H., Orme-Johnson W. H., 1979. Iron-Sulfur Clusters in the Molybdenum-Iron Protein Component of Nitrogenase. Electron Paramagnetic Resonance of the Carbon Monoxide Inhibited State. *Biochemistry*, **1**, 4860-4869.
- [12] Kumar P., Lee H. N., Kumar R., 2014. Synthesis of Phase Pure Iron Oxide Polymorphs Thin Films and Their Enhanced Magnetic Properties. *Journal of Materials Science: Materials in Electronics*, **25**, 4553–4561.
- [13] Carter E. A., Hargreaves M. D., Kononenko N., Howell G. I., Edwards G. M., Swarbrick B., Torrence R., 2009. Raman Spectroscopy Applied to Understanding Prehistoric Obsidian Trade, in the Pacific Region. *Vibrational Spectroscopy*, **50**, 116-124.
- [14] Hanesch M., 2009. Raman Spectroscopy of Iron Oxides and (oxy)Hydroxides at Low Laser Power and Possible Applications in Environmental Magnetic Studies. *Geophysical Journal International*, **177**, 941-948.
- [15] Wang L., Lu X., Han C., Lu R., Yang S., Song X., 2014. Electrospun Hollow Cage-like α -Fe₂O₃ Microspheres: Synthesis, Formation Mechanism, and Morphology-preserved Conversion to Fe Nanostructures. *Crystal Engineering Communications*, **16**, 10618–10623.
- [16] Neale A. R., Jin Y., Ouyang J., Hughes S., Hesp D., Dhanak V., Dearden G., Edwardson S., Hardwick L. J., 2014. Electrochemical Performance of Laser Micro-structured Nickel Oxyhydroxide Cathodes. *Journal of Power Sources*, **271**, 42-47.
- [17] Yoon H., Xu A., Sterbinsky G. E., Arena D. A., Wang Z., Stephens P. W., Meng Y. S., Carroll K. J., 2015. In Situ Non-aqueous Nucleation and Growth of Next Generation Rare-earth-free Permanent Magnets. *Physical Chemistry Chemical Physics*, **17**, 1070-1076.
- [18] Namduri H., Nasrazadani S., 2008. Quantitative Analysis of Iron Oxides Using Fourier Transform Infrared Spectrophotometry. *Corrosion Science*, **50**, 2493–2497.